Bioorganic & Medicinal Chemistry Letters 21 (2011) 5493–5497

Contents lists available at ScienceDirect

Bioorganic & Medicinal Chemistry Letters

journal homepage: www.elsevier.com/locate/bmcl

Identification of pyridazin-3-one derivatives as potent, selective histamine H_3 receptor inverse agonists with robust wake activity

Robert L. Hudkins *, Lisa D. Aimone, Thomas R. Bailey, Robert J. Bendesky, Reddeppa reddy Dandu, Derek Dunn, John A. Gruner, Kurt A. Josef, Yin-Guo Lin, Jacquelyn Lyons, Val R. Marcy, Joanne R. Mathiasen, Babu G. Sundar, Ming Tao, Allison L. Zulli, Rita Raddatz, Edward R. Bacon

Discovery Research, Cephalon, Inc., 145 Brandywine Parkway, West Chester, PA 19380, USA

ARTICLE INFO

Article history:
Received 26 May 2011
Revised 23 June 2011
Accepted 24 June 2011
Available online 30 June 2011

Keywords:
Histamine H_3
H_3 inverse agonist
CEP-26401
Pyridazin-3-one
Sleep–wake

ABSTRACT

H_3R structure–activity relationships on a novel class of pyridazin-3-one H_3R antagonists/inverse agonists are disclosed. Modifications of the pyridazinone core, central phenyl ring and linker led to the identification of molecules with excellent target potency, selectivity and pharmacokinetic properties. Compounds **13** and **21** displayed potent functional H_3R antagonism in vivo in the rat dipsogenia model and demonstrated robust wake activity in the rat EEG/EMG model.

© 2011 Elsevier Ltd. All rights reserved.

Histamine elicits physiological responses mediated by four G-protein coupled receptors (H_1R–H_4R) and exerts a variety of functions in the central nervous system (CNS).[1] H_1 and H_2 receptors in the periphery are involved in the allergic response and gastric acid secretion, respectively, and have been some of the more successful drug target classes over the past 50 years. The H_4 receptor is expressed mainly in mast cells, eosinophils, and tissues involved in the immune response, and may play a role in inflammation and pain.[2] The H_3 receptor (H_3R) in the brain is primarily localized presynaptically, where it functions both as an autoreceptor to modulate histamine release and as an inhibitory heteroreceptor regulating the release of multiple neurotransmitters, including acetylcholine (ACh), dopamine (DA), norepinephrine (NE) and serotonin (5-HT).[1] While activation of the H_3R results in the inhibition of neurotransmitter release, blockade of H_3R by selective antagonists or inverse agonists can reverse the histamine-mediated inhibition of neurotransmitter release, leading to enhanced release. H_3Rs by virtue of their localization and function regulate a variety of neurotransmitters that are thought to be involved in attention, sleep and cognition.[1c–i] The discovery of H_3R antagonists are of current interest, with potential utility in addressing a variety of CNS disorders associated with attention and cognitive deficits, including deficits in wakefulness, attention–deficit hyperactivity disorder (ADHD), Alzheimer's disease (AD), mild cognitive impairment, and schizophrenia. Several clinical candidates (Ia–Ie) have advanced into trials (Fig. 1).[1g–m]

We identified a novel class of pyridazin-3-one H_3R antagonists/inverse agonists with exceptional drug properties, safety and in vivo profiles.[3] The preliminary structure–activity relationships (SAR) and characterization of **1** (CEP-26401, irdabisant) and N-methyl **2** were recently disclosed.[4] In this paper we report SAR around the pyridazinone core, central phenyl ring and the linker leading to the identification of molecules with excellent target

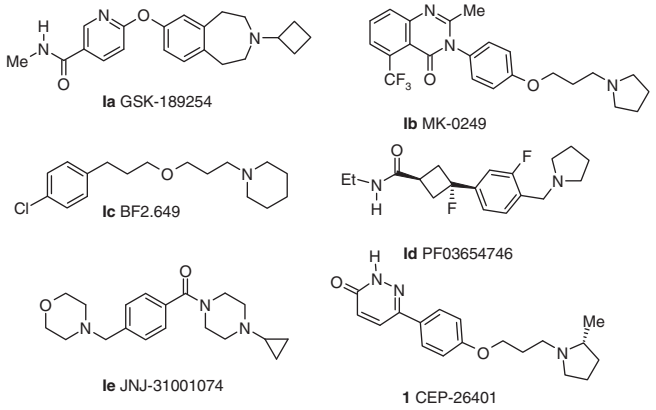

Figure 1. Structures of clinical H_3R antagonists.

* Corresponding author. Tel.: +1 610 738 6283.
E-mail address: rhudkins@cephalon.com (R.L. Hudkins).

0960-894X/$ - see front matter © 2011 Elsevier Ltd. All rights reserved.
doi:10.1016/j.bmcl.2011.06.108

potency and selectivity, pharmacokinetic properties and potent in vivo wake-promoting activity in the rat.

The N^2-substituted targets (e.g. **3–8**) were synthesized using our previously described method outlined in Scheme 1.[3,4] Cyclocondensation of 4-(4-methoxyphenyl)-4-oxobutyric acid **23** (or ester) with (N-substituted)hydrazine,[5a] oxidation of the resulting 4,5-dihydropyridazinone **24** (MnO_2, $CuCl_2$ or SeO_2/HOAc) to **25**,[5b] followed by O-demethylation produced phenol intermediates **26** in very good yield and purity. Alkylation of **26** with 3-bromo-1-chloropropane provided chloroalkyl intermediates that were reacted with R-2-methylpyrrolidine to produce targets **3–8**. In an analogous manner, ring substituted analogues (e.g. **13–18**) were synthesized starting with a phenyl substituted keto-acid or ester **23**. An alternative approached was employed for 3-cyano **19** using a previously described Suzuki coupling. 5-Boranyl-2-[3-((*R*)-2-methyl-pyrrolidin-1-yl)-propoxy]-benzonitrile with 3,6-dichloropyridazine and hydrolysis of the intermediate chloropyridazine gave **19**.[4] The *S*- and *R*-methyl linker isomers **21** and **22** were synthesized by alkylation of 26 (R^2 = Me, R^1 = H) with *R*- and *S*-3-bromo-2-methyl-propanol to provide **27**, conversion to the mesylate then (*R*)-2-methylpyrrolidine alkylation (Scheme 1). Synthesis of the central ring 3-pyridyl **20** was produced by ethyl 4-(6-chloropyridin-3-yl)-4-oxo-butyrate **28** and hydrazine hydrate cyclization to the 4,5-dihydro-2H-pyridazinone **29**, followed by alkylation with 3-(*R*-2-methylpyrrolidin-1-yl)propan-1-ol using DMSO and base to directly produce aromatized target **20** (Scheme 2). The 4-methyl analogue **9** was synthesized by the procedure outlined in Scheme 1, starting with 4-(4-methoxyphenyl)-3-methyl-4-oxobutyric acid.

Additional approaches to selectively modify either the 4- or 5-position are shown in Schemes 3–5. The 5-methyl analogue **11** was produced using a modification of our previously described

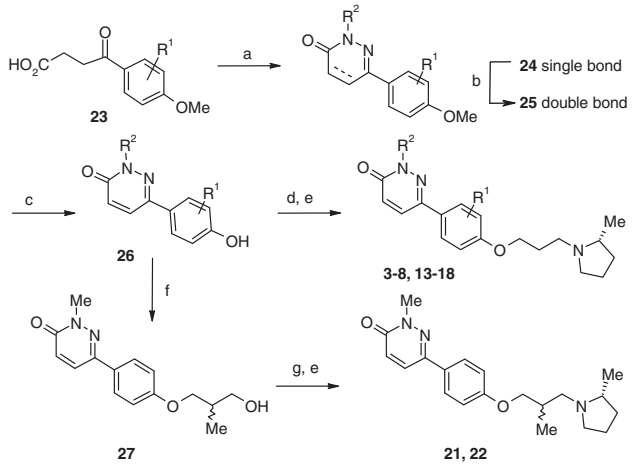

Scheme 1. Reagents and conditions: (a) R^2NHNH_2, 2-propanol, reflux, 80–95%; (b) MnO_2, xylenes, 155 °C, SeO_2/HOAc or Cu(II)Cl_2, CH_3CN, reflux, 50–85%; (c) BBr_3, DCM, 5 °C → rt, 70–95%; (d) K_2CO_3, $Br(CH_2)_3Cl$, acetone, 65 °C; (e) (*R*)-2-methylpyrrolidine, NaI, K_2CO_3, CH_3CN 80 °C, 35–60% two steps; (f) *R* or *S* 3-bromo-2-methylpropanol, K_2CO_3, CH_3CN 80 °C, 50–75%; (g) (i.) MsCl, TEA, DCM; (ii.) (*R*)-2-methylpyrrolidine, NaI, K_2CO_3, CH_3CN 80 °C, 40–60% two steps.

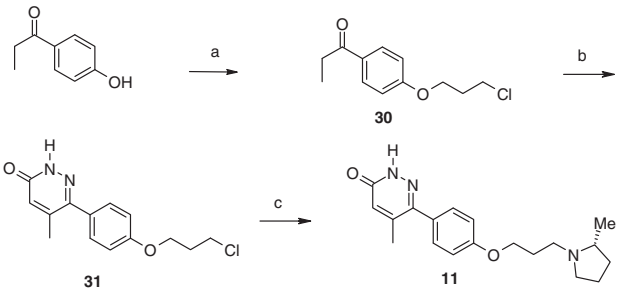

Scheme 3. Reagents and conditions: (a) $Br(CH_2)_3Cl$, K_2CO_3, acetone, 80 °C. 65%; (b) (i.) HC(O)COOH·H_2O, 85 °C; (ii.) NH_2NH_2·H_2O, ethanol, 85 °C. two steps 35%; (c) *R*-2-methylpyrrolidine, K_2CO_3, CH_3CN; 67%.

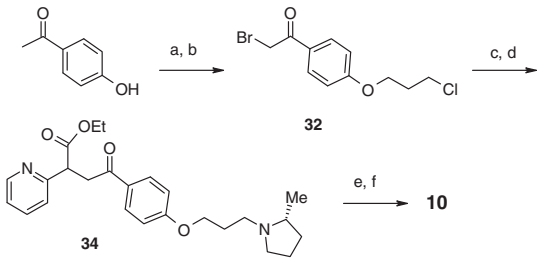

Scheme 4. Reagents and conditions: (a) K_2CO_3, $Br(CH_2)_3Cl$, acetone, 80 °C, 70%; (b) CuBr, EtOAc, $CHCl_3$, reflux, 70%; (c) ethyl 2-pyridylacetate, NaH, DMF, 72% → 33; (d) (*R*)-2-methylpyrrolidine, NaI, K_2CO_3, CH_3CN 80 °C; (e) NH_2NH_2·H_2O; ethanol, HOAc, 46%; (f) DMSO, K_2CO_3, 80 °C, 75%.

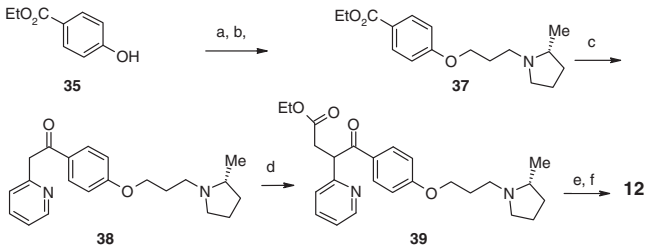

Scheme 5. Reagents and conditions: (a) K_2CO_3, $Br(CH_2)_3Cl$, acetone, 80 °C, 89% → 36; (b) (*R*)-2-methylpyrrolidine, NaI, K_2CO_3, CH_3CN 80 °C, 96%; (c) LiHMDS, THF, 2-methylpyridine, 0 → 45 °C, 70–80%; (d) NaH, $BrCH_2CO_2Et$, DMSO, toluene, 52%; (e) NH_2NH_2·H_2O; ethanol, 25%; (f) NaOH, water, EtOH, Na 3-nitrobenzenesulfonic acid, 35%.

Aldol/hydrazine cyclocondensation sequence to construct the pyridazinone ring[4,6] (Scheme 3).

Chloro **30** was condensed with glyoxalic acid monohydrate in acetic acid at 135 °C, followed by hydrazine cyclocondensation of the resulting Aldol adduct to give the 4,5-dihydro-2H-pyridazin-3-one **31** in low yield. Incorporation of (*R*)-2-methylpyrrolidine gave **11**. The critical step toward the synthesis of the 4-pyridyl **10** (Scheme 4) was alkylation of 2-bromo-1-[4-(3-chloropropoxy)phenyl]ethanone **32** with ethyl 2-pyridinyl acetate to produce

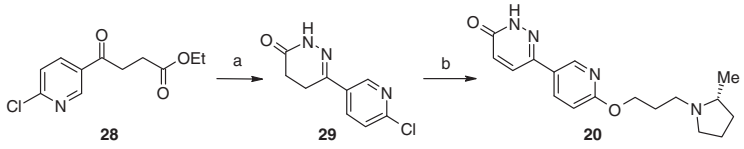

Scheme 2. Reagents and conditions: (a) H_2NNH_2·H_2O, ethanol, 80 °C, 87%; (b) 1 M KtOBu, t-BuOH, 3-(*R*-2-methylpyrrolidin-1-yl)propan-1-ol, DMSO, 100 °C, 8%.

33 (72% yield). Installation of (*R*)-2-methylpyrrolidine (**34**), hydrazine cyclization, followed by DMSO oxidation produced **10** in 30% yield. The 5-(2-pyridyl) **12** synthesis commenced with ethyl 4-hydroxybenzoate **35** (Scheme 5), installation of the amine side chain (**36** → 37), and 2-methylpyridine addition to ketone **38**, followed by subsequent alkylation with ethyl bromoacetate to produce the keto-ester intermediate **39**. Hydrazine condensation and oxidation of the 4,5-dihydropyridazinone using sodium 3-nitrobenzenesulfonate produced **12**.

The pyridazinone analogues were tested using in vitro binding assays by displacement of [^{3}H]NAMH in membranes isolated from CHO cells transfected with cloned human H_3 or rat H_3 receptors as shown in Table 1 and Table 2.[3,4] The (*R*)-2-methylpyrrolidine amine was previously established to be optimum[4] and was fixed for comparison while exploring further SAR. Also previously disclosed was substitution at the N^2 position could accommodate significant steric bulk without affecting H_3R binding affinity, although increasing the size of the R^2 group greater than methyl (**2**) resulted in compounds with log *P* values greater than **3**. This negatively affected molecular weight and decreased the ligand efficiency (LE) and the ligand lipophilic efficiency (LLE).[7] Amphiphilic, high log *P* compounds have been shown to enhance hERG activity and drive high tissue distribution inducting phospholipidosis.[8] Motivated to synthesize compounds with lower *c* log *P*, the fluorinated ethyl (**3** and **4**) and polar N-ethanol **5** were designed. Similar to other simple alkyl derivatives (e.g. **2**)[4] compounds **3**, 4 and **5** also had high affinity for both human and rat H_3R. Further discovery flow profiling with these analogues however showed poor oral bioavailability in the rat ($F < 10\%$). Lowering the *c* log *P* also was the motivation for replacement of the lipophilic R^2 phenyl **6** with more polar 2-pyridyl **7** and 2-pyrimidinyl **8** heteroaryls. The 2-Pym **8** showed balanced and slightly higher affinity compared with **7** for both human and rat H_3Rs (hH_3R K_i = 1.4 nM, rH_3R K_i = 7.9 nM) with lower lipophilicity (calculated *c* log *P* = 1.8 by the Tripos method). Compound **8** had acceptable in vitro metabolic stability across species in liver microsomes ($t_{½}$ > 40 min in mouse, rat, dog, monkey and human) and IC_{50} values > 30 μM for inhibition of cytochrome P450 enzymes CYP1A2, 2C9, 2C19, 2D6 and 3A4, indicating minimal potential for drug–drug interactions. In a hERG patch–express assay **8** had an IC_{50} value >10 μM. Compound 8 also showed excellent selectivity (>1000-fold) for hH_1, hH_2, and hH_4 receptor subtypes and against a panel of 70 GPCRs, ion channels and enzymes. In a rat pharmacokinetic experiment **8** showed acceptable i.v. intrinsic pharmacokinetic properties ($t_{½}$ = 1.5 h, CL = 29 mL/min/kg, V_d = 3.9 L/kg) and oral bioavailability (F = 56%). However, the brain exposure was low (brain/plasma ratio (B/P) = 0.5) for potential CNS indications, and this compound was not further advanced. Subsequently, the 4- and 5-positions were probed with methyl and 2-Pyr substitution. Methyl substitutions (**9** and **11**) were equally tolerated at both positions, while the 5-Pyr 12 had 4-fold and 7-fold lower affinity for hH_3R and rH_3R, respectively, compared to the 4-Pyr **10**. Compounds 10 and **12** showed acceptable in vitro metabolic stability, but did not show improvement in oral bioavailability (F < 10%) and/or brain exposure (B/P << 1) compared to **1** or **2**.

Table 1
Pyridazin-3-one H_3R binding data[a,b]

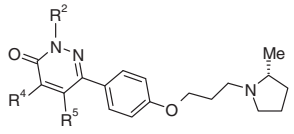

Entry	R^2	R^4	R^5	hH_3 (K_i nM)	rH3 (K_i nM)	*c* log *P*
1	H	H	H	2.0 ± 0.4	7.2 ± 0.4	2.3
2	Me	H	H	1.4 ± 0.1	6.3 ± 1.1	2.8
3	CH_2CH_2F	H	H	3.4 ± 0.5	11 ± 0.5	2.6
4	CH_2CF_3	H	H	5.7 ± 0.8	11 ± 0.5	2.7
5	CH_2CH_2OH	H	H	3.0 ± 0.1	9.5 ± 0.7	1.5
6	Ph	H	H	2.5 ± 0.9	7.9 ± 1.6	4.3
7	2-Pyr	H	H	10 ± 2	22 ± 3	2.8
8	2-Pym	H	H	1.4 ± 0.1	7.9 ± 0.8	1.9
9	H	Me	H	3.4 ± 0.1	8.7 ± 1.0	2.8
10	H	2-Pyr	H	3.1 ± 0.03	10 ± 1.0	3.1
11	H	H	Me	2.9 ± 0.1	12 ± 0.1	2.5
12	H	H	2-Pyr	12 ± 1	70 ± 1	2.3

[a] K_i values nM ± SEM.
[b] Pyr = 2-pyridine; 2-Pym = 2-pyrimidine.

Table 2
Pyridazin-3-one central ring and linker H_3R binding data[a]

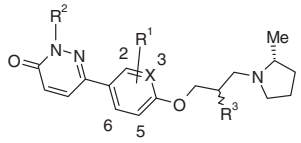

Entry	R^1	R^2	X	R^3	hH_3 (K_i, nM)	rH_3 (K_i, nM)
13	3-F	Me	C	H	5.8 ± 1.2	27 ± 7
14	2-F	H	CH	H	16 ± 2	69 ± 24
15	3-Cl	Me	C	H	4.4 ± 0.5	14 ± 2
16	3,5-F	Me	C	H	11 ± 3	41 ± 5
17	3,5-F	H	C	H	7.1 ± 1.4	40 ± 4
18	2-OMe	H	CH	H	152 ± 19	229 ± 65
19	3-CN	H	C	H	38 ± 12	111 ± 17
20	H	H	N	H	35 ± 14	70 ± 15
21	H	Me	CH	S-Me	2.4 ± 0.4	4.6 ± 1
22	H	Me	CH	R-Me	15 ± 2	52 ± 5

[a] K_i values nM ± SEM.

Data in Table 2 reveals the effect of varying the substitution on the central phenyl ring. Substitution in the 3-position with fluorine (**13**), chlorine (**15**) or with 3,5-difluoro (**16**, and **17**) were tolerated for H_3R binding affinity, while 2-substitution showed significantly reduced H_3R affinity (e.g. **14** and **18**). Replacing the central phenyl ring with 3-pyridyl **20** led to $a \geqslant$ 10-fold decrease in human and rat H_3R affinity. The effect of incorporating a chiral methyl group on the propyl linker was also investigated with *S*-21 and *R*-22. The *S*-isomer 21 retained hH_3R (K_i = 2.4 nM) and rH_3R (K_i = 4.6 nM) affinity equivalent to **2**, while *R*-22 had 6- and 11-fold weaker affinity for hH_3R and rH_3R.

Based on target affinity and physical property data (pH2 and pH7.4 solubility >0.25 mg/mL, *c* log *P* = 3.3 and 3.0) *S*-methyl 21 and 3-fluoro 13 were further profiled for selectivity against hH_1, hH_2, and hH_4 receptor subtypes and against a panel of 70 GPCRs, ion channels and enzymes (MDS Pharma Services, LeadProfiler). Compound 13 showed <30% inhibition against hH_1, hH_2, and hH_4 subtypes at 10 μM concentration, and inhibited only the norepinephrine transporter (NET) by greater than 70% at 10 μM concentrations in the broader screening panel. Compound 21 also showed excellent selectivity (> 1000-fold) for hH_1, hH_2, and hH_4 subtypes and displayed <30% inhibition at 10 μM concentration in the MDS panel of 70 targets, including NET (19% inh.). Functionally, 13 and 21 showed potent antagonist activity and displayed full inverse agonist activity in the [^{35}S]GTPγS hH_3R binding assay.[3,4] 3-Fluoro 13 and *S*-Methyl 21 decreased basal activity with EC_{50} values of 1.3 ± 0.1 nM and 2.1 ± 0.1 nM, respectively.

Based on the target H_3R affinity, selectivity, in vitro metabolic stability in liver microsomes ($t_{½}$ > 40 min across species) and CYP inhibition selectivity (IC_{50} > 30 μM), **21** and **13** were further evaluated for pharmacokinetic properties in the rat (Table 3) in comparison with **2**.[4] Compound 13 showed an i.v. $t_{½}$ of 1.2 h, clearance of 38 mL/min/kg, and oral bioavailability of 42% based on 6 h

AUC data with good brain exposure (B/P = 3.4). *S*-Me 21 had similar oral bioavailability (%*F* = 37 based on 6 h AUC) with good brain exposure in the rat (B/P = 2.5) (Table 3).

The rat dipsogenia model was used in the project as an in vivo surrogate measure of H_3R functional inhibition in the brain following peripheral administration. Histamine and the H_3-selective agonist, *R*-α-methylhistamine (RAMH), induce water drinking in the rat when administered either peripherally or centrally, an effect that is blocked by H_3R antagonists.[1h,9] In this model both **13** and **21** potently and dose-dependently inhibited RAMH-induced dipsogenia with ED_{50} values of 0.13 (0.02–0.91) mg/kg i.p. and 0.02 (0.005–0.07) mg/kg i.p., respectively. Following the demonstration of potent in vivo H_3R functional activity in the brain, **13** and **21** were further evaluated for wake promoting activity in the rat.[10] Histamine-producing neurons are an important part of the monoaminergic arousal system and H_3R antagonists have been documented to increase wakefulness in a number of species, although at doses and cortical H_3R occupancy levels much higher than those producing activity in the dipsogenia model or efficacy in cognition models.[11] Wake promoting activity was measured as previously described using male Sprague Dawley rats surgically implanted for chronic recording of EEG (electroencephalographic) and EMG (electromyographic) signals.[12] The cumulative wake time at 4 h after dosing was evaluated during the normal quiet period of the rat. Compound **21** increased waking at **3** (166 ± 6 min) and 10 mg/kg i.p. (231 ± 6 min) by 4 h AUC values ($P < 0.001$ ANOVA). At 10 mg/kg, waking was enhanced out to 5.5 h post dosing, and maximal cumulative wake surplus was 196 min reached at 7 h. EEG activity, behavior and body temperature were all normal at the 3 or 10 mg/kg doses. At 10 mg/kg, **21** demonstrated robust wake promotion, with the treated animals being awake 96% of the time up to 4 h post dose and averaging a 62% increase in wake time over the vehicle treated animals (Fig. 2). Compound **13** increased wake activity in a dose-related manner at **10** (157 ± 9 min) and 30 mg/kg (184 ± 15 min) by 4 h AUC values ($P < 0.001$ ANOVA) (Fig. 3). Compound **13** showed less robust wake activity compared to **21**, consistent with weaker potency in the dipsogenia model.

Table 3
Pharmacokinetic properties in rat[a]

		2[b]	**13**[b]	**21**[c]
i.v.	$t_{1/2}$/(h)	1.6 ± 0.3	1.2 ± 0.3	0.8 ± 0.2
	V_d (L/kg)	6.5 ± 2.9	4.5 ± 1.4	2.5 ± 1.0
	CL (mL/min/kg)	45 ± 11	38 ± 7	37 ± 8
p.o	AUC (ng h/mL)	538 ± 75	936 ± 166	892 ± 198
	C_{max} (ng/mL)	123 ± 6	284 ± 34	146 ± 9
	$t_{1/2}$/(h)	2.3	1.6	4.3
	F (%)	28 ± 4	42 ± 7	38 ± 8
	B/P[d]	3.5 ± 0.4	3.4 ± 0.3	2.5 ± 0.1

[a] Administration at 1 mg/mg i.v. and 5 mg/kg p.o.; data calculated from 6 h AUC values.
[b] i.v. formulation (3% DMSO, 30% solutol, 67% phosphate buffered saline) oral formulation (saline).
[c] i.v. formulation (3% DMSO, 30% solutol, 67% phosphate buffered saline) oral formulation (50% Tween 80, 40% propylene carbonate and 10% propylene glycol).
[d] B/P = brain to plasma ratio.

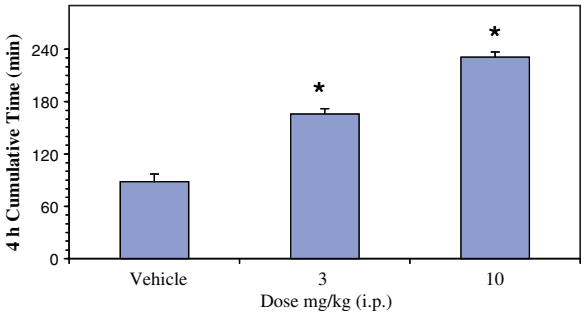

Figure 2. Compound **21**-induced wake promotion; administered i.p. to male rats chronically implanted with electrodes for recording EEG and EMG activity. Cumulative wake 4 h AUC values shown for each dose (mean + SEM, $n = 7–8$/group). $^*p < 0.05$ Dunnett's post hoc versus vehicle.

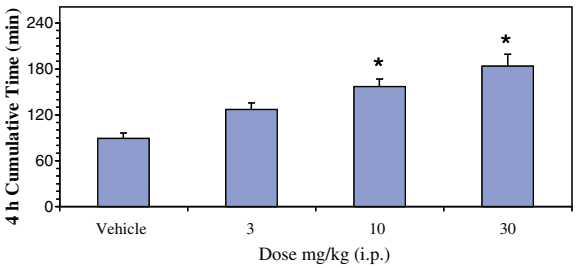

Figure 3. Compound **13**-induced wake promotion; administered i.p. to male rats chronically implanted with electrodes for recording EEG and EMG activity. Cumulative wake 4 h AUC values shown for each dose (mean + SEM, $n = 7–8$/group). $^*p < 0.05$, Dunnett's post hoc versus vehicle.

In summary, H_3R structure-activity relationships were disclosed on the pyridazin-3-one phenoxypropyl amine core leading to the identification of new molecules displaying excellent H_3R target potency, selectivity and rat pharmacokinetic properties. Compounds **13** and **21** were profiled in greater detail and advanced into in vivo evaluations. Both compounds displayed potent H_3R antagonist activity in the brain using the rat dipsogenia model as a functional H_3R readout and demonstrated potent wake-promoting activity in the rat EEG/EMG model.

References and notes

1. For reviews see: (a) Berlin, M.; Boyce, C. W.; de Lera Ruiz, M. *J. Med. Chem.* **2011**, *54*, 26; (b) Brown, R. E.; Stevens, D. R.; Haas, H. L. *Prog. Neurobiol.* **2001**, *63*, 637; (c) Leurs, R.; Bakker, R. A.; Timmerman, H.; de Esch, I. J. *Nat. Rev. Drug Discovery* **2005**, *4*, 107; (d) Wijtmans, M.; Leurs, R.; de Esch, I. *Expert Opin. Investig. Drugs* **2007**, *16*, 967; (e) Esbenshade, T. A.; Fox, G. B.; Cowart, M. D. *Mol. Interv.* **2006**, *6*, 77; (f) Esbenshade, T. A.; Browman, K. E.; Bitner, R. S.; Strakhova, M.; Cowart, M. D.; Brioni, J. D. *Br. J. Pharmacol.* **2008**, *154*, 1166; (g) Hudkins, R. L.; Raddatz, R. *Ann. Rep. Med. Chem.* **2007**, *42*, 49; (h) Raddatz, R.; Tao, M.; Hudkins, R. L. *Curr. Top. Med. Chem.* **2010**, *10*, 153; (i) Brioni, J. D.; Esbenshade, T. A.; Garrison, T. R.; Bitner, S. R.; Cowart, M. D. *J. Pharmacol. Exp. Ther.* **2011**, *336*, 38; (j) Medhurst, A. D.; Atkins, A. R.; Beresford, I. J.; Brackenborough, K.; Briggs, M. A.; Calver, A. R.; Cilia, J.; Cluderay, J. E.; Crook, B.; Davis, J. B.; Davis, R. K.; Davis, R. P.; Dawson, L. A.; Foley, A. G.; Gartlon, J.; Gonzalez, M. I.; Heslop, T.; Hirst, W. D.; Jennings, C.; Jones, D. N.; Lacroix, L. P.; Martyn, A.; Ociepka, S.; Ray, A.; Regan, C. M.; Roberts, J. C.; Schogger, J.; Southam, E.; Stean, T. O.; Trail, B. K.; Upton, N.; Wadsworth, G.; Wald, J. A.; White, T.; Witherington, J.; Woolley, M. L.; Worby, A.; Wilson, D. M. *J.Pharmacol. Exp. Ther.* **2007**, *321*, 1032; (k) Nagase, T.; Mizutani, T.; Ishikawa, S.; Sekino, E.; Sasaki, T.; Fujimura, T.; Ito, S.; Mitobe, Y.; Miyamoto, Y.; Yoshimoto, R.; Tanaka, T.; Ishihara, A.; Takenaga, N.; Tokita, S.; Fukami, T.; Sato, N. *J. Med. Chem.* **2008**, *51*, 4780; (l) Thompson Reuters Integrity, Bavisant, entry 470497, 2011.; (m) Thompson Reuters Integrity, MK-0249, entry 433171, 2011.
2. (a) Leurs, R.; Chazot, P. L.; Shenton, F. C.; Lim, H. D.; de Esch, I. J. *Br. J. Pharmacol.* **2009**, *157*, 14; (b) Zampeli, E.; Tiligada, E. *Br. J. Pharmacol.* **2009**, *157*, 24; (c) Bhatt, H. G.; Agrawal, Y. K.; Raval, H. G.; Manna, K.; Desai, P. R. *Mini Rev. Med. Chem.* **2010**, *10*, 1293.
3. Bacon, E. R.; Bailey, T. R.; Becknell, N. C.; Chatterjee, S.; Dunn, D.; Hostetler, G. A.; Hudkins, R. L.; Josef, K. A.; Knutsen, L.; Tao, M.; Zulli, A. L.; US2010273779, 2010.
4. Hudkins, R. L.; Raddatz, R.; Tao, M.; Mathiasen, J. R.; Aimone, L. D.; Becknell, N. C.; Prouty, C. P.; Knutsen, L.; Yazdanian, M.; Moachon, G.; Ator, M. A.; Mallamo, J. P.; Marino, M. J.; Bacon, E. R.; Williams, M. *J. Med. Chem.* **2011**, *54*, 4781.
5. (a) Curran, W. V.; Ross, A. *J. Med. Chem.* **1974**, *17*, 273; (b) Sotelo, E.; Ravina, E. *Syn. Comm.* **2000**, *30*, 1.
6. (a) Wermuth, C. G.; Schlewer, G.; Bourguignon, J. J.; Maghioros, G.; Bouchet, M. J.; Moire, C.; Kan, J. P.; Worms, P.; Biziere, K. *J. Med. Chem.* **1989**, *32*, 528; (b) Coates, W. J.; McKillop, A. *Synthesis* **1993**, 334.

7. (a) Hopkins, A. L.; Groom, C. R.; Alex, A. *Drug Discovery Today* **2004**, *9*, 430; (b) Lesson, P. D.; Springthorpe, B. *Nat. Rev. Drug Discovery* **2007**, *6*, 881; (c) Perola, E. *J. Med. Chem.* **2010**, *53*, 2986.
8. (a) Ploemen, J. P.; Kelder, J.; Hafmans, T.; van de Sandt, H.; van Burgsteden, J. A.; Saleminki, P. J.; van Esch, E. *Exp. Toxicol. Pathol.* **2004**, *55*, 347; (b) Reasor, M. J.; Hastings, K. L.; Ulrich, R. G. *Expert Opin. Drug Saf.* **2006**, *5*, 567.
9. Clapham, J.; Kilpatrick, G. J. *Eur. J. Pharmacol.* **1993**, *232*, 99.
10. Lin, J. S.; Sergeeva, O. A.; Haas, H. L. *J. Pharmacol. Exp. Ther.* **2011**, *336*, 17.
11. Le, S.; Gruner, J. A.; Mathiasen, J. R.; Marino, M. J.; Schaffhauser, H. *J. Pharmacol. Exp. Ther.* **2008**, *325*, 902.
12. (a) Edgar, D. M.; Seidel, W. F. *J. Pharmacol. Exp. Ther.* **1997**, *283*, 757; (b) Opp, M. R.; Krueger, J. M. *Brain Res.* **1994**, *639*, 57.